Electron and anion mobility in low density hydrogen cyanide gas. I. Dipole-bound electron ground states

Th. Klahn and P. Krebs

Citation: The Journal of Chemical Physics **109**, 531 (1998); doi: 10.1063/1.476969
View online: http://dx.doi.org/10.1063/1.476969
View Table of Contents: http://scitation.aip.org/content/aip/journal/jcp/109/2?ver=pdfcov
Published by the AIP Publishing

Electron and anion mobility in low density hydrogen cyanide gas. I. Dipole-bound electron ground states

Th. Klahn and P. Krebs[a]
Institut für Physikalische Chemie und Elektrochemie, Lehrstuhl für molekulare physikalische Chemie, Universität Karlsruhe, Kaiserstrasse 12, D-76128 Karlsruhe, Federal Republic of Germany

(Received 3 September 1997; accepted 31 March 1998)

We measured the mobility of excess electrons in the polar hydrogen cyanide gas ($D = 2.985$ D) at low densities as a function of density and temperature by the so-called pulsed Townsend method. Experiments were performed at 294 and 333 K in the gas number density range $1.23\times10^{17} \leqslant n \leqslant 3.61\times10^{18}\ \mathrm{cm}^{-3}$. We found a strong density dependence of the ''zero-field'' density-normalized mobility (μn). Only about 10% of the observed density variation can be qualitatively explained by coherent and incoherent multiple scattering effects. With increasing gas density an increasing number of linear HCN dimers is formed which due to the high dipole moment ($D = 6.552$ D) represent much stronger electron scatterers than the HCN monomers. It was found that the dimers may be only in part responsible for the observed density effect. Therefore, we consider a transport process where short-lived *dipole-bound electron ground states* (lifetime $\geqslant 12$ ps) as quasilocalized states are involved. For comparison the electron mobility in *saturated* 2-aminoethanol vapor with a dipole moment of similar size ($D = 3.05$ D) does not show any anomalous density behavior in the temperature range $298 \leqslant T \leqslant 435$ K. In contrast to this the electron mobility in *saturated* but also in *nonsaturated* CH_3CN gas ($D = 3.925$ D) shows a density behavior similar to that in HCN. © *1998 American Institute of Physics.* [S0021-9606(98)01626-2]

I. INTRODUCTION

Slow electrons drifting under the influence of an external electric field E in polar gases undergo strong scattering due to the long-range anisotropic electron/electric dipole interaction.[1] For polar gases with a dipole moment $D \approx 3$ D the number density n at which the de Broglie wavelength just exceeds the mean free path of the electron is low, i.e., in the order of some $10^{19}\ \mathrm{cm}^{-3}$ at $T = 300$ K. Therefore, multiple scattering has to be considered already at much lower densities. In addition, it cannot be excluded at all that the electron is temporarily or permanently captured by the dipole molecules forming molecular negative ions. The probability of such a process increases with n. Therefore, the electron mobility in polar gases may show a large dependence on n and T at such low gas densities.

Molecular negative ions formed by electron addition to closed shell neutral molecules are frequently unstable relative to autodetachment. However, if the electric dipole moment of the molecule is sufficiently large then an electron may be captured in the electrostatic dipole field of the molecule to form a so-called dipole-bound anion. It were Fermi and Teller[2] who first established the critical permanent electric dipole moment $D_c = 1.625$ D required to bind an electron. Crawford and Delgarno,[3] Crawford and Garrett,[4] and Garrett[5] have shown that the electric dipole field of a stationary molecule can bind an electron in an infinite number of bound states if D is greater than D_c. The electron exists in an extensive orbital, described by a diffuse wave function.[6] The consideration of rotational degrees of freedom in real molecular systems has a rather strong effect on the critical binding properties of polar molecules: The number of bound states of the electron in the dipolar field of a molecule with $D > D_c$ is reduced to a finite number as it was shown by Garrett.[7] However, the minimum dipole moment necessary to support at least *one* bound state is increased by 10% to 30% in comparison with that of a dipole fixed in space. In this case D_c depends on the effective dipole length, the rotational state, and the moments of inertia of the polar molecules.[8]

The binding energies of dipole-bound electron states may be extremely small at least in cases where the dipole moment is near the critical value. Thus one could expect that the formation of the dipole-supported anion might be difficult to observe since the very diffuse and weakly bound electron would be subject to stripping by thermal collisional processes within a gas sample and/or by the electric fields to which they are subjected in the process of mass analysis or in drift mobility measurements. For example, such a dipole-bound anion in water, i.e., $(H_2O)_2^-$ was prepared by Haberland and co-workers in a beam experiment and detected by mass spectroscopy.[9] The vertical detachment energy of the water dimer anion of 42 meV was determined by photoelectron experiments by Bowen and co-workers.[10]

We are concerned with the electron transport processes in *polar* gases, especially in the transition from the quasifree to the localized electron state. In the past we have performed extensive electron mobility measurements in sub- and supercritical NH_3[11,12] and in subcritical H_2O[12,13] gas as a function of gas density and temperature up to very high densities in order to study this transition in a disordered medium of di-

[a] Author to whom correspondence should be addressed.

pole scatterers. We continued these studies on electrons in sub- and supercritical CH_3OH gas[14–16] and in subcritical CH_3CN[17] gas also at much lower densities to study different multiple scattering effects on the electron mobility. From preliminary and not very accurate results on the electron mobility in low density *saturated* CH_3CN vapor ($D=3.925$ D) we suggested that we have found dipole-bound electron ground states *in thermal equilibrium* (we prefer to use the formula $[e^{-}\cdots CH_3CN]$ instead of CH_3CN^{-} to point out the weakly bound electron) which are involved in the transport process.[14] In the meantime we have performed electron mobility measurements in low density CH_3CN gas with much higher accuracy which besides multiple scattering effects demonstrate the existence of short-lived dipole-bound electron states with a mean lifetime of about 20 ps ($303\leqslant T \leqslant 343$ K) as precursors of the localized electron states.[18] This result is supported by recent beam experiments performed by Schermann and coworkers[19] showing that Compton's method[20] for the production of dipole-supported $[e^{-}\cdots CH_3CN]$ could be used as a general way to get *ground state* dipole-bound anions. With this method electrons are attached to closed shell polar molecules from laser-excited Rydberg atoms. Subsequently, Schermann and co-workers field detached the dipole-bound electron from the produced anion $[e^{-}\cdots CH_3CN]$ to ensure that it possessed in fact a weakly bound diffuse electron as expected for the dipole-bound species. Such it has become now possible to compare qualitatively nonequilibrium results of beam experiments with thermal equilibrium results of mobility measurements.

The dipole moment $D=2.985$ D of HCN[21] is much smaller than that of CH_3CN but far above D_c. Therefore, HCN should form a dipole-bound electron state as predicted theoretically by Garrett.[6] Moreover, the influence of the dipole-bound state should be more easily observed in electron mobility measurements in comparison with CH_3CN because due to the lower dipole moment the contribution of incoherent multiple scattering effects should be quite small. However, in contrast to CH_3CN some complications are to be expected due to orientational correlations among the HCN molecules and/or due to HCN dimer formation. In a preliminary report we have given some hint to the formation of dipole-bound electrons in low density HCN gas.[22] In this paper we present an extensive study of the mobility of electrons in HCN gas. For comparison we present also results on the electron mobility in 2-aminoethanol, a molecule with a dipole moment similar to that of HCN but with larger moments of inertia.

In Sec. II we will give a description of our experiments. The experimental results are presented and discussed in Sec. III. There, we analyze the electron mobility observed in low density HCN gas according to Polischuk's theoretical calculations on quantum multiple scattering corrections to the mobility of the electrons.[23,24] It will be demonstrated, at least qualitatively, that due to the real behavior of the dipolar gas correlations in positions between the dipole molecules cannot be neglected. These effects, however, do not describe the observed density variation of the electron mobility. Therefore, we estimate also the influence of HCN dimers in the drift gas on the electron mobility in the single scattering

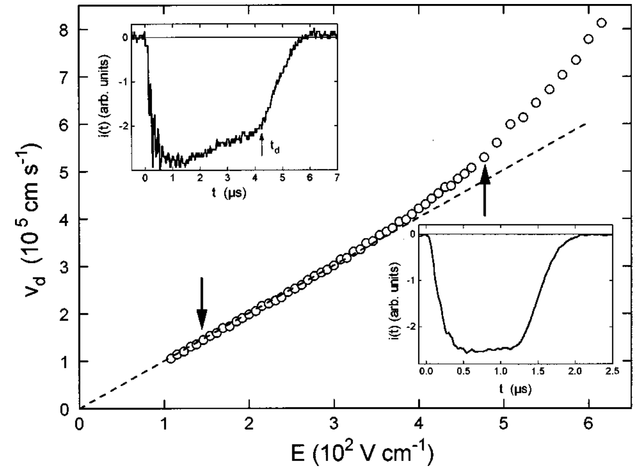

FIG. 1. Swarm drift velocity v_d as a function of the electric field strength E for electrons in low density HCN gas ($T=294$ K, $n=1.73\times 10^{18}$ cm^{-3}). The insets show the recorded electron current waveforms for different electric field strengths signed by the arrows. A part of the electrons is captured during the drift by HCN forming anions. The dashed line demonstrates the linear relationship between v_d and E at low electric field strength.

event approximation. Finally, we consider an effective electron localization process involving the dipole-bound state to take part in the electron transport. A summary is given in Sec. IV.

II. EXPERIMENT

A. Pulsed Townsend method

The pulsed Townsend method is a well-known and widely used method to perform electron mobility measurements. A constant potential difference U is applied between two circular, plane, parallel electrodes of radius r, separated by a distance d. A thin slice of n_e electrons is photoinjected from the cathode by means of a short UV laser pulse into the medium under investigation. Under the influence of the applied electric field $E=U/d$ the swarm of about 10^5 to 10^7 electrons drifts to the anode with the drift velocity v_{d} giving rise to an induced current $i=-en_e v_{\mathrm{d}}/d$ through a load resistor R_{L}, if $d\ll r$. If electron attachment to the gas molecules can be neglected, n_e and v_{d} are constant. In this simple case the (constant) current drops to zero when all the electrons are collected by the anode. With the experimentally observed electron current pulse duration t_d one obtains the drift velocity $v_{\mathrm{d}}=d/t_{\mathrm{d}}$. From the experimental linear relationship between v_{d} and E, the mobility μ is determined from $\mu=v_{\mathrm{d}}/E$ in the limit of zero field (see Fig. 1). In Fig. 2 we show the schematics of the experimental set-up for the electron and ion mobility measurements in HCN gas. For the electron mobility measurements in *low density* HCN gas we have developed a new drift cell (see Fig. 3). This drift cell is made out of Duran glass with quartz windows, and an electrode assembly made out of stainless steel. The distance d between the photocathode and the anode can be varied between 0.10 and 0.65 ± 0.01 cm. This cell withstands pressures up to 40 bar for temperatures $T\leqslant 400$ K. Different pressure sensors (Hottinger Baldwin) can be coupled to the drift cell to measure the gas pressure in the drift space with a

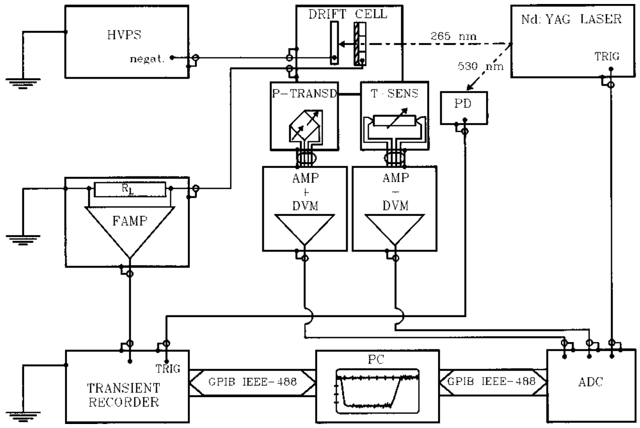

FIG. 2. Schematics of the apparatus for the pulsed photoinjection swarm experiments: Drift cell (see Fig. 3); P-TRANSD, different pressure transducers (Hottinger Baldwin); T-SENS, different temperature sensors; AMP +DVM, amplifier and digital voltmeters; HVPS, high-voltage dc power supply, Keithley Instruments 246; R_L, load resistor; FAMP, fast amplifier (homebuilt); Nd:YAG laser, J.K. Lasers, System 2000; PD, photodiode for triggering; Transient Recorder, Iwatsu DM 901; PC, personal computer; ADC, analog/digital converter (see the text).

maximum error of ± 0.6 mbar for the gas pressure range $p \leqslant 200$ mbar and of ± 2.5 mbar for $p \leqslant 1$ bar. The drift cell is also provided with a reservoir for about 10 ml of the medium under investigation.

B. Sample preparation[25]

1. Hydrogen cyanide

The production of HCN was performed according to a method described in Ref. 26, however, the procedure was stepwise improved in our laboratory. In the beginning about 24 g KCN were dried and degassed at 373 K at a vacuum line (better than 10^{-6} mbar). After KCN was cooled down to 77 K about 10 ml of fourfold distilled water were condensed on KCN. To avoid an undesired hydrolysis the KCN/water mixture was kept frozen until starting the synthesis. Subsequently, 30 ml of an aqueous solution of H_2SO_4 (50 mass %) were prepared in a dropping funnel and were gently bubbled with nitrogen (Messer Griesheim, 5.0) for at least 30 min to remove O_2 and other gases. Finally, the sulfuric acid was evacuated down to its own vapor pressure. Then the sulfuric acid was dropped on the stirred KCN/water mixture at 283 K. Starting at about 12 mbar (water vapor pressure) the vapor pressure increases due to the production of HCN gas. At about 100 to 200 mbar a valve was opened and HCN (under constant pressure conditions) was condensed in a trap cooled down to 77 K. Drying of the raw HCN was performed by trap-to-trap-sublimation at the vacuum line. Each trap was filled with freshly prepared P_2O_5.[27] Thereafter, P_2O_5 was added to hydrogen cyanide and it was refluxed for several hours for further purification and drying. Finally, HCN was fractionally distilled from the residues in a special glass apparatus under a nitrogen atmosphere through a 30 cm Vigreux column. The middle fraction (about 30%) was collected and kept in a reservoir attached to the vacuum line. HCN was degassed by several ''freeze–pump–thaw'' cycles and stored under its vapor pressure on twofold sublimated P_2O_5. It is well-known that small traces of water in HCN produce after some time brown and black condensates. However, hydrogen cyanide purified by our above mentioned method does not change during months at room temperature.

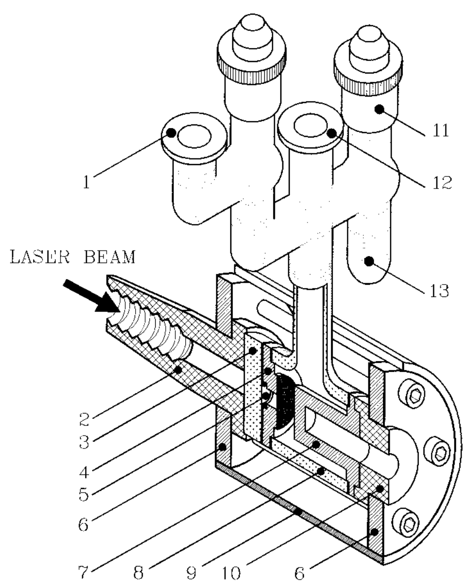

FIG. 3. Drift cell (for gas pressures up to 40 bar for T$\leqslant$400 K): 1, flange for the connection to the vacuum line; 2, PTFE conical adapter for adjustment of the drift cell in the steel tank; 3, quartz plate as optical window; 4, anode covered with a light transparent stainless steel mesh; 5, PTFE-O-sealing; 6, stainless steel flanges which hold together all the parts of the photocell; 7, photocathode; 8, cell vessel made out of duran glass; 9, shielding against electromagnetic irradiation; 10, PTFE centric adapter; 11, high vacuum valve (Young); 12, flange for the pressure transducer; 13, reservoir for the medium under investigation.

2. 2-aminoethanol

C_2H_7NO was purified by us in the following manner: 2-aminoethanol (Aldrich, 99%) was gently bubbled with argon (Messer Griesheim, 5.0); thereafter with a small amount of KBH_4 (Fluka) it was refluxed for at least 3 h under reduced pressure. Then it was fractionally distilled from the residues through a 30 cm Vigreux column. The middle fraction (about 30%) was collected and kept in a reservoir attached to the vacuum line. The reservoir was protected against irradiation of light.

3. Preparation of the sample in the drift cell

The drift cell was connected to the vacuum line in order to fill its reservoir with the medium under investigation. In the case of HCN the necessary amount of HCN was carefully sublimated in the reservoir. During this process the temperature of the main storage vessel for HCN at the vacuum line was held constant at 252 K. Before starting the mobility measurements, HCN in the drift cell reservoir was again made free of electron scavengers such as O_2 and CO_2 by several freeze–pump–thaw cycles. It should be pointed out that all parts of the apparatus which came in contact with HCN (or C_2H_7NO), in particular the drift cell, are cleaned with several organic solvents and were finally rinsed with overheated water vapor for at least 24 h.

At higher temperatures hydrogen cyanide shows autopolymerisation: A black charcoal-like substance is produced which is called ''azulmin.''[28] To avoid this effect we have tested many inhibitors mentioned in the literature.[29] Very effective was only cobaltoxalate ($CoC_2O_4 \cdot 2H_2O$, Aldrich).[30] Cobaltoxalate was ground and suspended in acetone (Merck, p.a.). For the high temperature measurements the drift cell was rinsed with this suspension. Then acetone was evaporated at the vacuum line. A small amount of solid cobaltoxalate was put also in the reservoir of the drift cell. Finally, the drift cell was dried and baked at 473 K at the vacuum line until there was formed a bluish colored coating on the glass surface due to cobaltoxalate.

The filled drift cell was then transferred into a steel tank filled with fine sand as a heat conducting medium. With an electrical heating system with PID-controllers (Eurotherm) the chosen temperature in the cell could be held constant to within ± 0.3 K. The temperature was measured by NiCr–Ni thermocouples and by platinum thermoresistors Pt 100 which were mounted on different positions at the drift cell. The gas pressure in the drift cell could be adjusted by carefully opening of a valve connected with the vacuum line or by controlled filling of the drift cell. With the measured gas pressure and temperature the number density n of HCN was determined from the approximated virial equation of state

$$n \approx \frac{2p}{k_B T}\left\{1+\left[1+\frac{4pB(T)}{N_A k_B T}\right]^{1/2}\right\}^{-1}, \tag{1}$$

with the second virial coefficient $B(T)$ taken from the literature.[31]

In the case of aminoethanol we have not found any virial coefficients in the literature. Therefore, we have estimated the density of the saturated vapor from the ideal gas equation. In the pressure range $0 \leqslant p \leqslant 1$ bar we have determined a maximum error of 5% to 10% at the boiling temperature ($T_b = 444$ K). At higher temperatures aminoethanol corrodes stainless steel. To avoid any additional complications concerning the drift cell and to avoid the damaging of the pressure sensors we have performed measurements only in the saturated vapor without this equipment. Therefore, the vapor pressures at the measured temperatures θ_T in centigrades were calculated from the Antoine equation

$$\log p = A^0 - \frac{B^0}{C^0 - \theta_T}, \tag{2}$$

with the parameters A^0, B^0, and C^0 taken from the literature.[31]

C. Signal wave forms

As the UV light source we used the fourth harmonic of a Nd:YAG laser (J.K. Lasers, System 2000: $\lambda = 266$ nm, pulse duration <20 ns, pulse energy <20 mJ). The induced photocurrent $i(t)$ produces a voltage drop $u(t)$ across the load resistor R_L which is amplified by a fast home-built amplifier. The output is fed to a transient recorder (Iwatsu DM 901, 5×10^7 samples/s) which is connected via an IEEE-488 bus interface to a personal computer. Signal accumulation was performed.

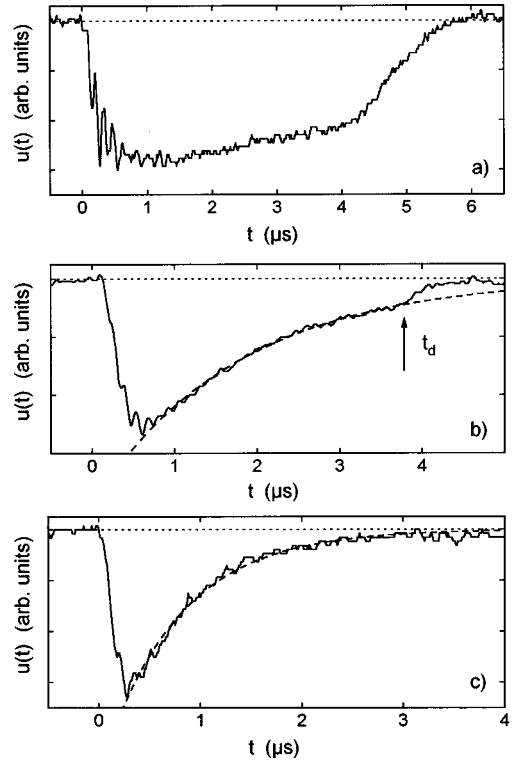

FIG. 4. Time dependent voltage wave forms of electrons in HCN gas as a function of the gas number density: (a) $n = 1.70\times 10^{18}$ cm^{-3}, $T = 294$K, $E = 1.533\times 10^2$ V cm^{-1}; (b) $n = 2.70\times 10^{18}$ cm^{-3}, $T = 333$ K, $E = 2.757\times 10^2$ V cm^{-1}; (c) $n = 3.90\times 10^{18}$ cm^{-3}, $T = 333$ K, $E = 6.126\times 10^2$ V cm^{-1}. The dashed lines in (b) and (c) are fitting time dependent exponential functions demonstrating the electron capturing process [see Eq. (3)].

Typical electronic wave forms $u(t)$ are shown in Fig. 4 for increasing HCN number densities n . If a short bunch of n_e^0 excess electrons is photoinjected in the drift space, the voltage drop $u(t)$ decreases during the drift time. In the ideal case it can be described by

$$\begin{aligned} u(t) &= -R_L \frac{e n_e^0}{t_d} \exp\{-t/\tau_e\} \quad 0 \leqslant t \leqslant t_d \\ &= 0 \quad t > t_d, \end{aligned} \tag{3}$$

where e is the elementary charge and τ_e is the mean lifetime of the excess electrons in the low density HCN ($k_{\text{eff}}^{(1)} = 1/\tau_e$ is the rate constant of disappearance of the electrons). In spite of the strong decay of $u(t)$ with time at $n = 2.7\times 10^{18}$ cm^{-3} the arrival of the electrons at the anode after the time t_d can be still observed [see Fig. 4(b)]. However, at number densities $n > 3.6\times 10^{18}$ cm^{-3} almost all the electrons are captured by HCN during the drift time [see, e.g., Fig. 4(c)]. This is observed for 294 K as well as for 333 K. We have also tried to measure electron mobilities at $T = 373$ K but under the present conditions the wave forms did not allow the determination of t_d due to the fast reaction of the electrons.

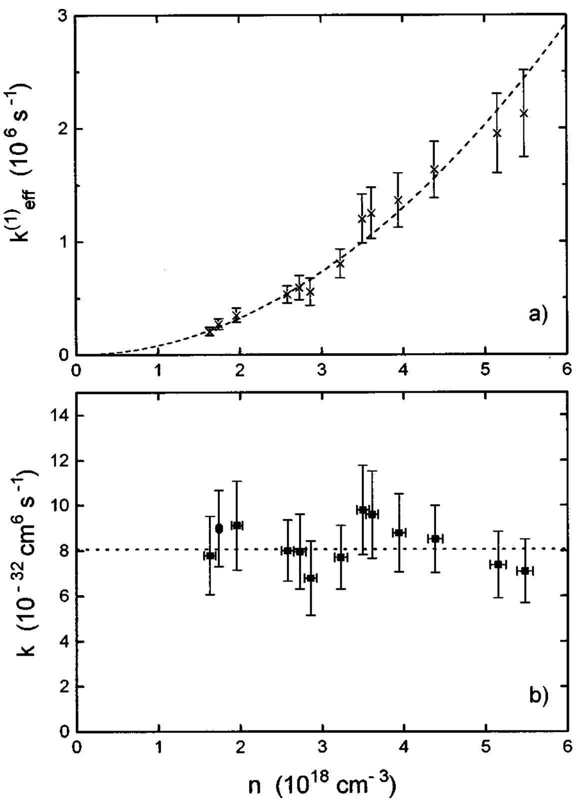

FIG. 5. (a) Rate constant $k_{\text{eff}}^{(1)}$ (of first order with respect to electrons) describing the disappearance of the electrons during the drift as a function of the HCN number density n for $T=333$ K: $\times$, experiment; the dashed line demonstrates the proportionality $k_{\text{eff}}^{(1)} \propto n^2$. (b) Rate constant for reaction (4), $k=k_{\text{eff}}^{(1)}/n^2$, as a function of n: ■, experiment; the dotted line shows the mean value of k.

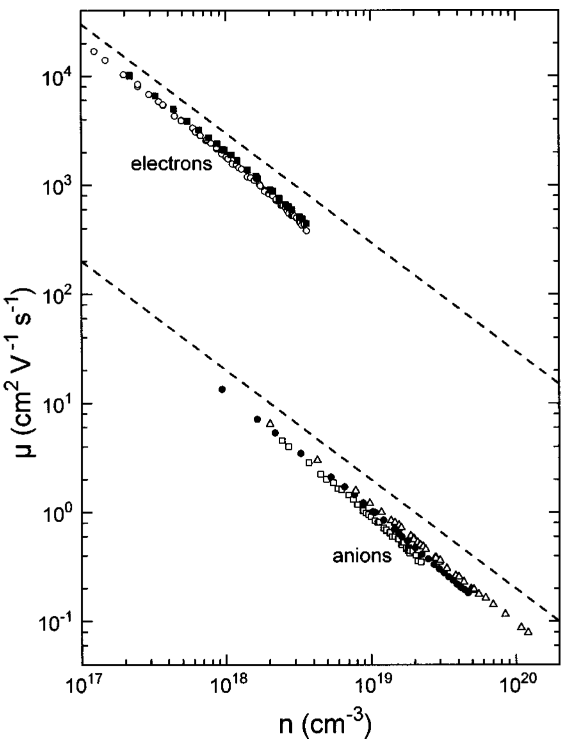

FIG. 6. Electron and anion mobilities in gaseous HCN as a function of n and T. Electron mobilities: ○, 294 K; ■, 333 K. Anion mobilities: □, 294 K; ●, 333 K; △, 373 K. The dashed lines show the classical $1/n$ density dependence.

III. RESULTS AND DISCUSSION

A. The kinetics of the reaction of electrons with HCN

We have analyzed the kinetics of the electron capturing process by fitting of Eq. (3) to the experimentally observed electronic wave forms. As can be seen from the fitting curves in Figs. 4(b) and 4(c) the disappearance of the electrons can be well described by an exponential function corresponding to a reaction of first order with respect to the electrons, i.e.,

$$e^- + j\ \text{HCN} \xrightarrow{k_{\text{eff}}^{(1)}} \text{A}^-. \tag{4}$$

A^- stands for some anionic species which is formed by the reaction of the electrons. In this overall reaction j HCN molecules may participate in the formation of the unknown species A^-. The rate constant determined by fitting of Eq. (3) to the experimental induced current profiles depends on the HCN gas density n. In Fig. 5(a) we show $k_{\text{eff}}^{(1)}$ as a function of n at 333 K. It follows from Figs. 5(a) and 5(b) that reaction (4) is second order with respect to HCN, i.e., $j=2$. Within the margins of the experimental errors one obtains for the rate constant $k=k_{\text{eff}}^{(1)}/n^2=(8\pm2)\times10^{-32}\text{cm}^6\ \text{s}^{-1}$. For a further discussion of this result we refer to paper II of this publication series.[32]

B. Electron and anion mobility

The electron mobility μ has been measured in the gas density range $1.23\times10^{17}\leq n\leq3.61\times10^{18}\ \text{cm}^{-3}$ for the temperatures 294 and 333 K. To give a survey on the experimental results of this investigation we present in Fig. 6 the mobility isotherms of the electrons for 294 and 333 K together with those of the anions for 294, 333, and 373 K (see also paper II of this publication series). Taking a first look on the electron mobility isotherms in the logarithmic representation one notes a much stronger density dependence than the classical $1/n$ behavior which was frequently assumed in the past by condensed matter physicists for such low gas densities.[33] This effect is better visualized when the "zero-field" density-normalized mobility (μn) is shown as a function of n in a *linear* representation (Fig. 7). For comparison, the classical behavior of the electron mobility is given for $T=333$ K by the horizontal dashed line. The overall experimental uncertainties of (μn) were estimated to be $\pm5\%$. Each mobility isotherm has been measured several times up and down to show the reproducibility of these measurements. It is generally noticed that the scatter of the very low density data is relatively high (see also Fig. 7 with the maximum calculated errors shown at some arbitrarily selected experimental points). The origin for this is at present unknown.

The observed strong density variation of (μn) will be discussed in the following section according to Polischuk's theoretical calculations on quantum density corrections to the mobility due to interference in multiple scattering and by taking into account also the imperfect gas behavior.

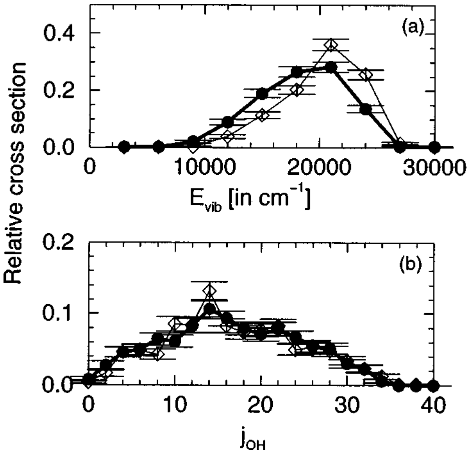

FIG. 7. Density-normalized mobilities (μn) of excess electrons in HCN gas as a function of number density n for 294 and 333 K. The solid lines are for the present guides for the eyes (see the text). The dashed line represents the classical result for 333 K. The error bars show the *maximum* calculated errors.

C. Multiple scattering corrections

The zero-field density-normalized mobility (μn) of multiple scattered electrons in an imperfect polar gas is given by[15,16]

$$(\mu n)\approx(\mu_{\mathrm{L}}n)\left\{1-\frac{\sqrt{\pi}}{8}(0.5\pi-0.6)\lambda\!\!\!^{-}_T\langle\sigma_{\mathrm{m}}^{\mathrm{av}}(\varepsilon)\rangle n + \frac{2B(T)}{N_A}n\ldots\right\}, \tag{5}$$

where ($\mu_{\mathrm{L}}n$) is the classical density-normalized mobility in the single collision approximation [Lorentz limit: see, e.g., Eq. (2) in Ref. 1]. ($\mu_{\mathrm{L}}n$) does not depend on the gas density. The first density correction on the right-hand side of Eq. (5) is due to quantum interference in multiple scattering which has been calculated by Polischuk.[23,24] This term is valid only at sufficiently low gas densities where the de Broglie wavelength $\lambda\!\!\!^{-}_T=\hbar/(2m_e k_{\mathrm{B}}T)^{1/2}$ of the thermal electrons is much smaller than their mean free path $L=1/\langle\sigma_{\mathrm{m}}^{\mathrm{av}}(\varepsilon)\rangle n$. $\langle\sigma_{\mathrm{m}}^{\mathrm{av}}(\varepsilon)\rangle$ is the thermal average of the theoretical momentum transfer cross section, $\sigma_{\mathrm{m}}^{\mathrm{av}}(\varepsilon)=(4\pi/3)(De/\hbar)^2 m_e/\varepsilon$, for dipole molecules in the point-dipole limit averaged over the dipole orientations ($\varepsilon=(\hbar k)^2/2m_e$ is the kinetic energy of the electron)[34]

$$\langle\sigma_{\mathrm{m}}^{\mathrm{av}}(\varepsilon)\rangle^{\mathrm{theor}}=Am_e/k_{\mathrm{B}}T \text{ with } A=(8\pi/3)(De/\hbar)^2. \tag{6}$$

The second term in Eq. (5) is a coherent multiple scattering correction due to positional correlations among the dipole scatterers in an imperfect gas. $B(T)$ is the second virial coefficient in units of $\mathrm{cm}^3\ \mathrm{mol}^{-1}$. Polischuk proposed to use in Eq. (5) the thermally averaged experimental cross section $\langle\sigma_{\mathrm{m}}^{\mathrm{av}}(\varepsilon)\rangle^{\mathrm{exp}}$ obtained from measurements at very low density[14,15]

$$\langle\sigma_{\mathrm{m}}^{\mathrm{av}}(\varepsilon)\rangle^{\mathrm{exp}}=\frac{8e}{3}(2/\pi m k_{\mathrm{B}}T)^{1/2}[(\mu n)_0]^{-1}, \tag{7}$$

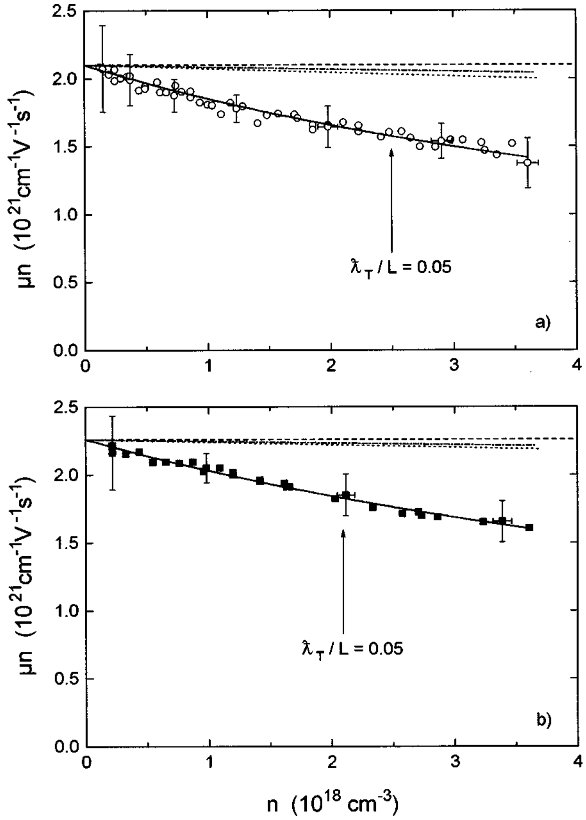

FIG. 8. Density-normalized mobility (μn) of electrons in HCN gas at 294 K (a), and 333 K (b) as a function of n in comparison with the results considering multiple scattering effects: solid lines connecting the experimental points have for the present no theoretical significance [they represent functions like $(\mu n)_0^{\mathrm{exp}}/(1+\mathrm{const.}\ n)$]; the dashed lines represent the classical result; the dashed-dotted lines show the density correction due to interference in multiple scattering [first correction term in Eq. (5)]; the dotted lines take into account additionally *coherent* multiple scattering effects due to the imperfect gas [complete Eq. (5)].

where $(\mu n)_0$ is the experimental zero-field density-normalized mobility in the limit of $n\rightarrow 0$. In this case ($\mu_{\mathrm{L}}n$) in Eq. (5) has to be replaced consequently by $(\mu n)_0$.

To compare the experimental results in HCN gas with theory we display in Fig. 8 the zero-field density-normalized mobility (μn) vs n for $T=294$ K and $T=333$ K. The dashed lines represent the classical result. To obtain $(\mu n)_0^{\mathrm{exp}}$ we have fitted the experimental points by a hyperbolic function of the type $(\mu n)_0^{\mathrm{exp}}/(1+\mathrm{const.}\ n)$ (the theoretical justification for this follows in Sec. III E). This was done also in Fig. 7. The thermal averaged experimental scattering cross sections are $\langle\sigma_{\mathrm{m}}^{\mathrm{av}}(\varepsilon)\rangle^{\mathrm{exp}}=2670\pm127\,\text{Å}^2$ ($T=294$ K) and $\langle\sigma_{\mathrm{m}}^{\mathrm{av}}(\varepsilon)\rangle^{\mathrm{exp}}=2341\pm135\ \text{Å}^2$ ($T=333$ K) which are distinctly smaller than the corresponding theoretical values $\langle\sigma_{\mathrm{m}}^{\mathrm{av}}(\varepsilon)\rangle^{\mathrm{theor}}=3473\ \text{Å}^2$ and $\langle\sigma_{\mathrm{m}}^{\mathrm{av}}(\varepsilon)\rangle^{\mathrm{theor}}=3066\,\text{Å}^2$ obtained from Altshuler's Eq. (6) (see also Fig. 9). With the experimental scattering cross section one can calculate the first correction term in Eq. (5). The result (dash–dotted lines in Fig. 8) shows that this is only a relatively small correction to the classical $(\mu n)_0$. However, even at such low HCN gas densities of the present investigation correlations between the scatterers cannot be neglected.[15] With the virial coefficients $B(T)$ of Table I one obtains from the *complete* Eq. (5) the dotted lines presented in Fig. 8. That means that both density corrections in

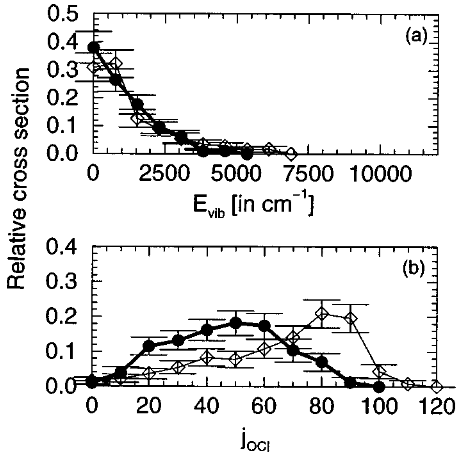

FIG. 9. Thermal averaged momentum transfer cross sections of polar molecules with respect to electrons vs the reciprocal temperature: ●, HCN ($T = 294$ and 333 K), this work; ×, aminoethanol, Hamilton and Stockdale (Ref. 58); ∇, aminoethanol, this work ($T=300$ K, see below). The dashed line shows a possible $1/T$ dependence of the experimental momentum transfer cross section. The solid line represents the theoretical result of Altshuler (Ref. 34) for $\bar{D}\approx 3.0$ D [Eq. (6)].

Eq. (5) are by far not sufficient to describe the density variation of (μn) in HCN. Concerning the orientational correlations in HCN gas we present in the following thermodynamic and spectroscopic evidence for significant formation of linear HCN dimers and their influence on the electron mobility.

D. The influence of HCN dimer formation on the electron mobility

1. The formation and properties of HCN dimers

Based on *PVT*-measurements performed on HCN in the thirties and forties of this century dimers and higher oligomers were postulated to exist in the gas phase.[35–37] Giauque and Ruehrwein[38] determined from *PVT*-data the equilibrium constant K_p for the dimerization reaction

$$2\mathrm{HCN} \overset{K_p}{\leftrightarrow} (\mathrm{HCN})_2 . \tag{8}$$

The dimensionless equilibrium constant K_p is defined by

$$K_p = \frac{p_D/p^0}{(p_M/p^0)^2} = \frac{p^0}{p_{\mathrm{tot}}}\frac{x_D}{(x_M)^2} \approx \frac{p^0}{p_{\mathrm{tot}}}\frac{x_D}{(1-x_D)^2}, \tag{9}$$

TABLE I. Zero-field density-normalized electron mobility $(\mu n)_0$ in HCN gas, scattering cross section $\langle \sigma_{\mathrm{m}}^{\mathrm{av}}(\varepsilon)\rangle^{\mathrm{exp}}$, and second virial coefficient $B(T)$ of HCN as a function of T (see the text).

T/K	$(\mu n)_0$/ 10^{21} cm^{-1} V^{-1} s^{-1} [a]	$\langle \sigma_{\mathrm{m}}^{\mathrm{av}}(\epsilon)\rangle^{\mathrm{exp}}$/ 10^{-13} cm^2 [b]	$B(T)$/ cm^3 mol^{-1} [c]
294	2.10 ± 0.10	2.670 ± 0.127	-1584.25
333	2.25 ± 0.13	2.341 ± 0.135	-913.92

[a] The errors are the maximum calculated errors determined by the method of error propagation. The standard deviation of the density normalized mobilities from the mean is $\leqslant 0.6\%$.
[b] Calculated with Eq. (7).
[c] Data from Ref. 31.

where p_i and x_i are the partial pressures and the mole fractions of the monomers (M) and dimers (D), p_{tot} is the sum of the partial pressures, and $p^0 = 1$ bar. Higher oligomers are neglected in the case when x_M is replaced by $(1-x_D)$. Giauque and Ruehrwein calculated K_p from the compression factor $Z = pV/nRT$ of HCN gas based on measurements of Sinosaki and Hara.[35] Giauque and Ruehrwein used for $p <$ 0.3 bar (where the measurements are not sufficiently accurate) the virial approximation $pV \approx RT\ (1 + B'(T)p)$; however, they employed the second virial coefficient of HCl [$B'(T_b) = -0.0056$ bar^{-1}, $T_b = 298.8$ K is the boiling temperature of HCN at 1 bar]. The equilibrium constant for the dimer formation at $T = 303$ K was obtained to be $K_p = -B'(303\ \mathrm{K})p_0 = 0.056$. From the temperature dependence of K_p they obtained the enthalpy of dimer formation $\Delta H_D^0 = -13.73$ kJ mol^{-1}, as well as the corresponding entropy change $\Delta S_D^0 = -69.04$ J K^{-1} mol^{-1}. Neglecting the formation of higher oligomers the mole fraction of the dimers, x_D, is a function of p_{tot}, i.e.,

$$x_D \approx 1 + \frac{p^0}{2K_p(T)p_{\mathrm{tot}}} - \left[\left(1 + \frac{p^0}{2K_p(T)p_{\mathrm{tot}}}\right)^2 - 1\right]^{1/2}. \tag{10}$$

Hyde and Hornig[39] were the first to show directly the existence of $(\mathrm{HCN})_2$ by infrared measurements. Jones, Seel, and Sheppard[40] studied $(\mathrm{HCN})_2$ by IR spectroscopy in the gas phase in more detail. The monomers are chain-like coupled caused by the large dipole moment of HCN and by a comparatively weak hydrogen bond interaction leading to an equilibrium N···C distance of the HCN dimer of $r_0(\mathrm{N\cdots C}) = 3.34 \pm 0.20$ Å. The standard enthalpy of formation was determined from the temperature dependent intensities of the absorption bands of the monomer and dimer to be $\Delta H_D^0 = -(23.85 \pm 2.10)$kJ mol^{-1} (see Table II.). In a further IR absorption study concerning $(\mathrm{HCN})_2$ in the gas phase at 300 K and a HCN gas pressure of up to 933 mbar Mettee[41] tried to verify spectroscopically the dimerization equilibrium constant K_p of Giauque and Ruehrwein. From constant volume measurements between 298 and 356 K (for $p \geqslant 933$ mbar) they obtained the internal energy of dimerization $\Delta U_D^0 = -15.90 \pm 0.67$kJ mol^{-1} and the corresponding dimerization enthalpy $\Delta H_D^0 = -(18.63 \pm 0.67)$kJ mol^{-1} and with ΔS_D^0 of Ref. 38 finally K_p (revised) = 0.40 for 303 K. The discrepancy between K_p (revised) = 0.40 and K_p (Ref. 38) = 0.056 was explained by Mettee to be due to an overestimate of the contributions of trimers and higher oligomers by Giauque and Ruehrwein by fitting the former vapor density data. HCN trimers have not been determined spectroscopically, neither by Jones *et al.* nor by Mettee. Using now the dimerization enthalpy of Jones *et al.* and the corresponding entropy term of Giauque and Ruehrwein one obtains for 300 K a much higher value for the equilibrium constant, i.e., $K_p = 3.45$. Of course, the strongly different dimerization equilibrium constants of Mettee and Jones *et al.* lead to compression factors which extremely differ from that of Giauque and Ruehrwein.

Concerning the structure and the dipole moment of $(\mathrm{HCN})_2$ we can rely on numerous experimental and theoretical investigations. Legon, Millen, and Mjöberg[42] have determined the rotational constant of the dimer in the gas phase

TABLE II. Summary of the properties of HCN dimers taken from the literature: Dipole moment D_D, equilibrium constant of dimerization K_p, rotational constant B_0, enthalpy of dimerization ΔH_D, and the equilibrium bond length r_0(N···C) of linear HCN dimers.

D_D/D	K_p[a]	B_0/MHz	ΔH_D/kJ mol^{-1}	r_0(N···C)/Å	Method	Ref.
···	0.056	···	−13.73	···	PVT	38
···	0.40	···	−18.63±0.67	···	IR	41
···	3.45	1709±120	−23.85±2.10	3.34±0.20	IR	40
···	···	1788.09±0.10	−14.8[b]	3.231	MW	42
6.0±0.5[c]	···	1788.214	···	···	MW	43
6.552±0.035[c]	···	···	···	···	FTMW	44
6.57–7.37	···	···	···	3.33–3.40	*ab initio*	45, 46
6.53–6.67	···	···	···	···	Pol[d]	47

[a]Calculated for $T=303$ K with $\Delta S_D^0=-69.04$ J K^{-1} mol^{-1} from Ref. 38.
[b]This value was calculated by the authors of Ref. 42 using different data from the literature.
[c]Stark-shift measurements.
[d]Consideration of mutual polarization of the monomers in the dimer.

($p_{\rm tot}=0.5$ Torr, $T=200$ K) to be $B_0=1788.09$ MHz. The calculated bond length r_0(N···C)=3.231 Å agrees quite well with r_0(N···C)=3.34±0.20 Å given by Jones *et al.* HCN dimers have also been studied by microwave spectroscopy by Brown *et al.*[43] which yields $B_0=1788.214$ MHz. From the observed Stark-shift it follows a dipole moment of the dimer $D_D=6.0\pm1.5$ D. Campbell and Kukolich[44] have investigated the dimer $(\mathrm{HC}^{15}\mathrm{N})_2$ in a molecular beam by the method of Fourier transform microwave spectroscopy and obtained $D_D=6.552\pm0.035$ D.

Ab initio calculations on a linear HCN dimer done by Kofranek *et al.*[45,46] yield a dipole moment between 6.57 and 7.37 D. The equilibrium bond length r_0(N···C) lies between 3.33 and 3.40 Å. The enthalpy of dimerization varies between −14.2 and −15.9 kJ mol^{-1}. Ruoff[47] has calculated the dipole moment of the HCN dimer considering additionally mutual polarization effects. He obtained values for D_D between 6.53 and 6.67 D. For a better survey we have collected all these quantities in Table II.

2. The influence of HCN dimers on the electron mobility

Because the scattering cross section depends approximately on the squared dipole moment it follows that the scattering cross section of the dimer $(\mathrm{HCN})_2$ should be by a factor of almost 5 larger than that of the HCN monomer. Depending on the concentration of $(\mathrm{HCN})_2$ the influence of the dimers on the electron mobility might be quite considerable. For example, based on the analysis of Giauque and Ruehrwein the mole fraction of the dimers at the boiling point 298.8 K ($p_{\rm tot}=1.01325$ bar) is $x_D=0.0494$.

In order to estimate the effect of HCN dimers on the electron mobility we "synthesize" a gas mixture consisting of monomers and dimers neglecting the relatively large contributions of all the higher oligomers of HCN (at $T_b=298.8$ K and $p_{\rm tot}=1.01325$ bar Giauque and Ruehrwein have determined besides x_D also $x_T=0.0089$, and $x_Q=0.0016$, etc.). Each of both components should behave like an ideal gas. On the basis of the *PVT* data of Giauque and Ruehrwein we obtain then a revised equilibrium constant $K_p^{\rm rev}=0.098$ at $T_b=298.8$ K ($p_{\rm tot}=1.01325$ bar) based on $x_D^{\rm rev}=0.0824$ obtained from the compression factor $Z=0.9239$. Defining a total number density n^* of this mixture

$$n^*=\frac{N_M+N_D}{V}=\frac{N_{\rm tot}}{V}=\frac{p_{\rm tot}}{k_{\rm B}T}, \tag{11}$$

one obtains from Eq. (10) the mole fraction x_D^* of the dimers in this artificial gas mixture as a function of $p_{\rm tot}$ and T

$$x_D^*=1+\frac{p^0}{2n^*k_{\rm B}TK_p^{\rm rev}(T)}-\left[\left(1+\frac{p^0}{2n^*k_{\rm B}TK_p^{\rm rev}(T)}\right)^2-1\right]^{1/2}, \tag{12}$$

where $K_p^{\rm rev}(T)$ can be calculated with the results of Giauque and Ruehrwein. This artificial monomer/dimer gas mixture behaves with respect to electrons like a mixture of differently strong polar scatterers. In order to calculate the total scattering cross section of the mixture we can take into account an ansatz of Christophorou *et al.*[48] used for a mixture of the nonpolar ethene and a polar gas

$$\langle\sigma_{\rm m}^{\rm av}(\varepsilon)\rangle^{\rm mix}=A^{\rm mix}m_e/k_{\rm B}T=(x_1A_1+x_2A_2)m_e/k_{\rm B}T. \tag{13}$$

Assuming that there are only *single scattering events* (Lorentz approximation) between the electron and the monomer or the dimer, respectively, we can apply Eq. (13) on our "mixture of two polar gases". The experimental scattering cross section $\langle\sigma_{\rm m}^{\rm av}(\varepsilon)\rangle^{\rm exp}$ of HCN was determined by extrapolation of the density-normalized mobility (μn) to $n\to0$. In this case it can be assumed that $\langle\sigma_{\rm m}^{\rm av}(\varepsilon)\rangle^{\rm exp}$ represents the thermally averaged cross section of the HCN monomers with respect to electrons. As mentioned above any deviation of the compression factor Z from $Z=1$ has been interpreted as being due to HCN dimer formation. Therefore, the former number density n has to be replaced by n^*. Within the presented experimental density range the quantities n and n^* differ by only 1%. With Eq. (6) the scattering cross section of the dimer can be approximately calculated from the scattering cross section of the monomer, $\langle\sigma_{\rm m}^{\rm av}(\varepsilon)\rangle^{\rm exp}$, i.e.,

$$\langle\sigma_{\rm m}^{\rm av}(\varepsilon)\rangle_D^{\rm exp}\approx(D_D/D_M)^2\langle\sigma_{\rm m}^{\rm av}(\varepsilon)\rangle^{\rm exp}. \tag{14}$$

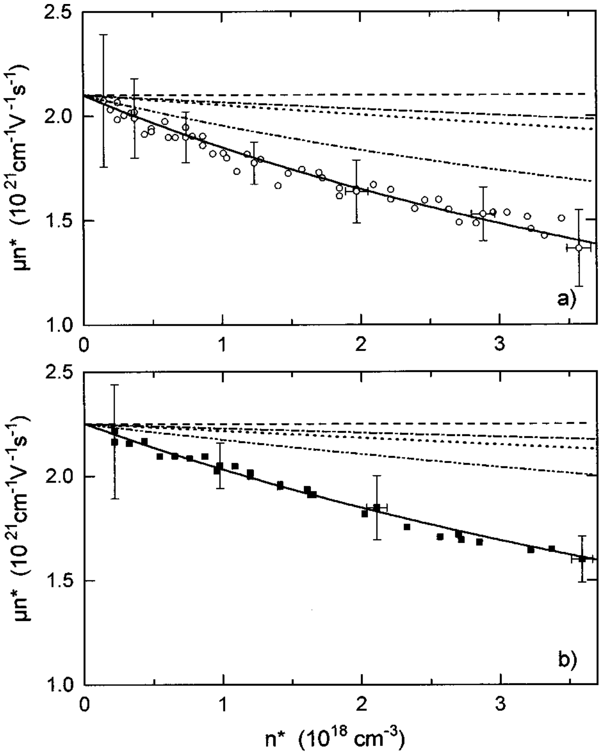

FIG. 10. Density-normalized mobility (μn^*) of electrons in HCN gas at 294 K (a), and 333 K (b) as function of the total number density n^* of the monomer/dimer gas mixture (see the text). Dashed lines: classical result; dashed-dotted lines: influence of HCN dimers [Eq. (16)] taking into account the revised equilibrium constant of Giauque and Ruehrwein $K_p^{\text{rev}}(294\ \text{K})=0.107$ and $K_p^{\text{rev}}(333\ \text{K})=0.055$; dashed-(two)-dotted line: influence of HCN dimers considering, however, the equilibrium constants of Mettee $K_p(294\ \text{K})=0.502$ and $K_p(333\ \text{K})=0.205$ [Eq. (16)]; dotted line: dimer formation (Giauque and Ruehrwein) and density correction due to interference in multiple scattering [Eqs. (5) and (16)]. Solid line: best fit of the dipole-bound electron state model [Eq. (17)] to the experimental points. The density-normalized mobility of the quasi-free electrons in this model has been calculated with the corresponding corrections due to incoherent multiple scattering and due to dimer formation.

Using Eq. (2) of Ref. 1 and Eqs. (13) and (14) one obtains the density-normalized electron mobility in the monomer/dimer gas mixture

$$(\mu n^*)^{\text{mix}}=\frac{8e}{3}[2(\pi m_e k_B T)]^{1/2}\{\langle\sigma_{\text{m}}^{\text{av}}(\varepsilon)\rangle^{\text{exp}} \times[x_D^*(D_D/D_M)^2+x_M^*]\}^{-1}. \tag{15}$$

With Eq. (7) and $x_M^*=1-x_D^*$ one finally has

$$(\mu n^*)^{\text{mix}}=(\mu n)_0\left[1+\left(\frac{D_D^2}{D_M^2}-1\right)x_D^*\right]^{-1}, \tag{16}$$

where the mole fraction of the HCN dimer, x_D^*, can be calculated with Eq. (12).

At the highest number density of this investigation on the electron mobilities the mole fraction of the HCN dimers is about 0.015. It follows that the influence of the dimers on the electron mobility at these low gas densities is relatively small in spite of the large scattering cross section (see Fig. 10). However, it should be emphasized that according to Fig. 10 this effect is larger than the density correction due to multiple scattering processes. It should be pointed out at this stage that considering multiple scattering effects we took into account only the incoherent correction (dotted line in Fig. 10). By neglecting the coherent multiple scattering correction depending on $B(T)$ we want to avoid that the effect of $B(T)$ leading to HCN dimers will be counted twice. To demonstrate the influence of the dimers on the electron mobility still more pronounced we have used instead of $K_p^{\text{rev}}(T)$ of Giauque and Ruehrwein also the very large equilibrium constant $K_p=0.40$ of Mettee. The dashed-(two)-dotted lines in Fig. 10 show that the density effect due to dimers depends very sensitively on the accuracy of the thermodynamic results on the HCN gas. The assumption that gaseous HCN at $T=294$ K consists only of monomers and dimers must be considered as an approximation. A small amount of trimers can have a nonnegligible influence on the electron mobility since the molecular beam FTMW experiments have shown linear trimers with a dipole moment of 10.61 D. However, we do not consider the influence of trimers and higher oligomers on the electron mobility due to the lack of sufficiently accurate data.

TABLE III. Experimental density-normalized electron mobilities, $(\mu n^*)_0^{\text{exp}}$, in the limit $n^*\to 0$ and the electron attachment/detachment equilibrium constant K as a function of temperature.

T/K	$(\mu n^*)_0^{\text{exp}}/10^{21}$ cm^{-1} V^{-1} s^{-1} [a]	$K/10^{-20}$ cm^3
294	2.10 ± 0.10	11.7 ± 0.8
333	2.25 ± 0.13	9.80 ± 0.88

[a]In the limit $n^*\to 0$ it follows that $(\mu n^*)_0^{\text{exp}}\equiv(\mu n)_0^{\text{exp}}$ (see Table I).

From Fig. 10 it is concluded that there must exist an additional density dependent scattering process or a localization process which is more effective than the weak localization due to interference in multiple scattering. In the following section we give another explanation for the density variation of the density-normalized mobility which is based on the concept of the so-called dipole bound electron ground state.

E. The dipole-bound electron ground state as a temporary localization center

Similar to the case of multiple scattered electrons e_f^- in CH_3CN gas[18] we show that the anomalous density dependence of the electron mobility in HCN can be described by the first term on the r.h.s. of the following expression for an oscillatory transport process (see the solid line in Fig. 10)[49–51]

$$\mu^{\text{eff}}n^*=\frac{\mu_f n^*}{1+Kn^*}+\frac{\mu_l K n^{*2}}{1+Kn^*} \tag{17}$$

with the constants $K(T)$ given in Table III. The mobility of the multiple scattered electrons, μ_f, has been determined by Eq. (16). The experimental result of Eq. (17) is in accordance with a dynamical electron attachment/detachment equilibrium

$$e_f^-+\text{HCN}\overset{K}{\leftrightarrow}[e^-\cdots\text{HCN}]_l \tag{18}$$

with the equilibrium constant $K(T)=k_{fl}/k_{lf}$. The attachment rate of the multiple scattered electron to HCN is given by $k_{fl}n^{*}=1/\tau_{fl}$ and the electron detachment from the quasilocalized electron state $[e^{-}\cdots\mathrm{HCN}]_l$ is determined by the rate constant $k_{lf}=1/\tau_{lf}$ (τ_{lf} is the mean lifetime of the quasilocalized electron state). The second term of Eq. (17) can be neglected in our case because for the quasilocalized state one has $\mu_l \ll \mu_f$. This equation is valid only if the drift time t_d is by many orders of magnitude larger than τ_{fl} and τ_{lf}.[49]

We assert now that $[e^{-}\cdots\mathrm{HCN}]_l$ represents a dipole-bound electron ground state. In the following we want to support this suggestion. First we are looking for some information on the time constant $\tau_{fl}=1/k_{fl}n^{*}$. Mothes *et al.*[52] have determined the low pressure attachment rate constant k_{fl} by the electron cyclotron resonance method, however, at much lower HCN gas densities ($n \leq 10^{12}$ cm^{-3}) in comparison with those of our swarm experiment. Without taking into account the possible detachment reaction they obtained $k_{fl}=9.1\times10^{-11}$ cm^3 s^{-1} at $T=290$ K. With this value we get from the equilibrium constant $K=11.7\times10^{-20}$ cm^3 at $T=294$ K and $n^{*}=1\times10^{18}$ cm^{-3} $\tau_{lf}\approx1.3$ ns and $\tau_{fl}\approx11$ ns. Both time constants seem to be not sufficiently small in comparison with the observed drift time of several hundred nanoseconds to about 5 μs as required by the oscillatory model. We conclude, therefore, that k_{fl} may be by several orders of magnitude larger than the above experimental estimate but the autodetachment rate constant is also very high so that the formation of *stable* $[e^{-}\cdots\mathrm{HCN}]_l$ could not be *directly* observed in swarm experiments. This was already suggested by Stockdale *et al.* in the case of electrons in CH_3CN.[20] Schermann and co-workers[19] studied charge transfer collisions between laser excited xenon (nf, np) Rydberg atoms and acetonitrile molecules and clusters. $[e^{-}\cdots\mathrm{CH_3CN}]_l$ has been observed in these supersonic expansion beam experiments only in narrow ranges of Rydberg n values. The attachment rate constant was found to be much higher, i.e., $k_{fl}=(1\pm0.5)\times10^{-8}$ cm^3 s^{-1}. This result has to be compared with the corresponding low pressure value $k_{fl}=7.2\times10^{-12}$ cm^3 s^{-1} of Mothes *et al.*[52] We use Schermann's rate constant as an *upper limit* for the interpretation of our results in HCN. This value and the equilibrium constant $K=(11.7\pm0.10)\times10^{-20}$ cm^3 obtained in our swarm experiment yield $\tau_{lf}\geq11.7$ ps and $\tau_{fl}\geq(1/n^{*})\times10^{-10}$ s, where the number density n^{*} has to be substituted in units of 10^{18} cm^{-3}. The calculated lifetimes of the electron in the different states are in fact much smaller than the experimentally observed drift times between at least 400 ns and a few microseconds in accordance with the conditions of the model.

Such an oscillatory transport process with the short lifetime τ_{lf} in the order of some tens picoseconds due to the detachment process is reasonable only if the binding energy of the quasilocalized electron is small, i.e., it should be comparable to the thermal energy. The electron binding energy was determined by Schermann and co-workers in the case of $[e^{-}\cdots\mathrm{CH_3CN}]_l$ by field detachment in the supersonic beam experiment. They obtained $E_b=-11.5$ meV.)[19,53] For comparison, the electron affinity E.A. ≈0.5 meV for CH_3CN was determined by an *ab initio* calculation by Jordan and Wendoloski.[54] The dipole moment of the neutral water dimer is known to be about 2.6 D,[55] and it binds an electron to form the dipole supported anion $[e^{-}\cdots(\mathrm{H_2O})_2]$. From field detachment experiments it follows an electron binding energy close to -9 meV[56] whereas photoelectron experiments measured the vertical detachment energy to be 42 meV.[10]

In the case of $[e^{-}\cdots\mathrm{HCN}]_l$ the binding energy should be comparable to those limiting values. Jordan and Wendoloski estimated E.A. ≈1 meV[54] whereas Garrett studied the permanent and induced dipole requirements in *ab initio* calculations of the electron affinity of HCN within the limits $1\leq$E.A.≤10 meV.[6] From the temperature dependence of the equilibrium constant K for the attachment/detachment equilibrium (18) one can get a measure for the binding energy. The relevant parameters are collected in Table III. From the results for 294 and 333 K one can realize a decrease of K with increasing temperature as it is expected. The van't Hoff equation (under the experimental condition $V=$const.) leads finally to an estimate of the internal energy change for the electron attachment reaction (formation of the dipole-bound state) $\Delta U=-(38\pm25)$meV corresponding to $\Delta U=-(1.52\pm0.98)N_Ak_\mathrm{B}T$ for $T=294$ K.

The proposed electron transport process with the temporary nondissociative dipole-binding of an electron by HCN is valid only in the gas density range where $\lambda\!\!\!^{-}_T \ll L$. From this interpretation it follows that the lifetime of $[e^{-}\cdots\mathrm{HCN}]_l$ of about 12 ps does not depend on n^{*} in the density range under investigation. This can be true only if with increasing density n^{*} (or n) the mean time interval between two molecular collisions is much larger than the lifetime of the dipole-bound state. This time was estimated to be in the order of 1 ns at the *highest* density of this investigation. Therefore, the lifetime of $[e^{-}\cdots\mathrm{HCN}]_l$ is obviously not controlled by molecular collisions as it was feared in the introduction of this paper.

F. Excess electrons in saturated aminoethanol vapor

Finally we present the results of the electron mobility measurements in *saturated* aminoethanol vapor in the temperature range $298\leq T\leq435$ K (Fig. 11). Despite the fact that its dipole moment $D=3.05$ D[57] is similar to that of HCN the density-normalized mobility does not show any anomalies (see the inset in Fig. 11). It should be emphasized, however, that the errors of these experiments are for the following reasons extremely large. On the one hand, temperature fluctuations lead sometimes to condensation of aminoethanol from the saturated gas phase on the photocathode surface thus changing the mobility. On the other hand, the lack of a useful equation of state for aminoethanol does not allow an accurate determination of the vapor number density. The extrapolation of the density-normalized mobility to $n\rightarrow0$ (see the dashed line in the insert of Fig. 11) leads to an estimate of the mean momentum transfer cross section $\langle\sigma_\mathrm{m}^\mathrm{av}(\varepsilon)\rangle^\mathrm{exp}\approx(2655\pm136)$ Å^2 which agrees quite well with $\langle\sigma_\mathrm{m}^\mathrm{av}(\varepsilon)\rangle^\mathrm{exp}=2661$ Å^2 determined by Hamilton and Stockdale[58] at 300 K (Fig. 9).

For comparison it should be mentioned that in contrast to the results in aminoethanol the density-normalized mobility in *saturated* CH_3CN vapor shows in spite of likewise

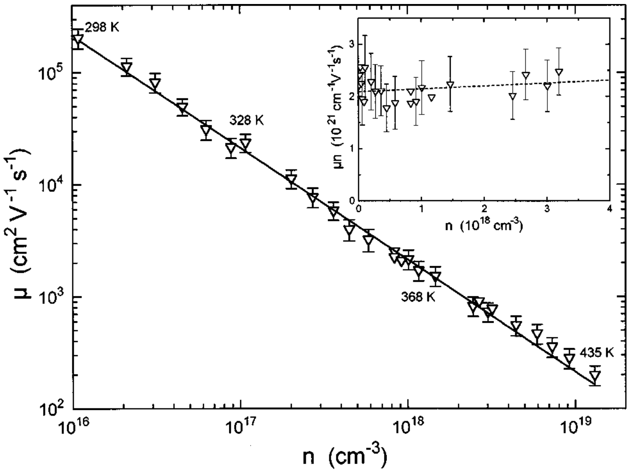

FIG. 11. Electron mobility in saturated aminoethanol vapor as a function of the vapor number density in the temperature range $298 \leqslant T \leqslant 435$ K. Some experimental points are signed with the corresponding temperature. The solid line serves as guide for the eye. The inset shows the density-normalized mobility as a function of n. The dashed line which was fitted to the experimental data points shows a slightly positive slope due to the temperature dependence of (μn).

large experimental errors an anomalous density variation of (μn) similar to that in HCN.[14] Acetonitrile tends to dimerize too but the dimers are characterized by a preferentially *anti-parallel* orientation of the monomers.[59] Thus this orientational correlation of CH_3CN dipoles cannot be responsible for the observed density dependence of (μn) in acetonitrile vapor.

Theoretical calculations of Garrett demonstrate that for molecules with comparable dipole moments the critical dipole moment D_c for the formation of the dipole-bound electron state is lower just for those molecules with higher moments of inertia.[8] Since the so-called dipole-length does not play a decisive role for the size of D_c it would follow that the dipole-bound state should be more easily observed in the case of aminoethanol than in HCN if we assume that the binding energy and the lifetime are comparable in both media. Therefore, if there exist one day sufficiently accurate measurements on the density-normalized mobilities in aminoethanol which in fact do exclude the existence of dipole-bound states then it is a challenge for the theoreticians to explain the observed behavior.

IV. SUMMARY

We have measured electron and anion mobilities in a wide range of densities and temperatures. The electron data have been analyzed carefully at those densities where the de Broglie wavelength is much smaller than the mean free path of thermal electrons. The density dependence of the density-normalized mobility can be explained neither by interference in multiple scattering nor by positional correlations among the dipole scatterers and orientational correlations (dimer formation) in the imperfect gas. We have argued that dipole-bound electron ground states where the electron is localized for at least twelve picoseconds in the dipole field of the slowly moving polar HCN molecule dominates the transport process.

ACKNOWLEDGMENTS

This work is dedicated to Professor U. Schindewolf. Support of this work by the Deutsche Forschungsgemeinschaft and by the Fonds der Chemischen Industrie is gratefully acknowledged.

[1] L. G. Christophorou and A. A. Christodoulides, J. Phys. B **2**, 71 (1969), and references therein.
[2] E. Fermi and E. Teller, Phys. Rev. **72**, 406 (1947).
[3] O. H. Crawford and A. Delgarno, Chem. Phys. Lett. **23**, 547 (1966), and references therein.
[4] O. H. Crawford and W. R. Garrett, J. Chem. Phys. **66**, 4968 (1977).
[5] W. R. Garrett, J. Chem. Phys. **77**, 3666 (1982).
[6] W. R. Garrett, J. Chem. Phys. **71**, 651 (1979).
[7] W. R. Garrett, Mol. Phys. **20**, 751 (1971).
[8] W. R. Garrett, J. Chem. Phys. **73**, 5721 (1980), and references therein.
[9] H. Haberland, in *The Chemical Physics of Atomic and Molecular Clusters,* Proceedings of the 106th International School ''Enrico Fermi'', Varenna 1988, edited by G. Scoles (North-Holland, Amsterdam, 1990), p. 619 and references therein.
[10] (a) K. H. Bowen and J. G. Eaton, in *The Structure of Small Molecules and Ions,* edited by R. Naaman and Z. Vager (Plenum, New York, 1988); (b) J. V. Coe, G. H. Lee, J. G. Eaton, S. T. Arnold, H. W. Sarkas, K. H. Bowen, C. Ludewigt, H. Haberland, and D. R. Worsnop, J. Chem. Phys. **92**, 3980 (1989).
[11] P. Krebs, V. Giraud, and M. Wantschik, Phys. Rev. Lett. **44**, 211 (1980).
[12] P. Krebs, J. Phys. Chem. **88**, 3702 (1984), and references therein.
[13] V. Giraud and P. Krebs, Chem. Phys. Lett. **86**, 85 (1982).
[14] Th. Klahn, P. Krebs, and U. Lang, in *Proceedings of a NATO Advanced Study Institute on Linking the Gaseous and Condensed Phases of Matter: The Behavior of Slow Electrons,* Vol. 326 Series B, edited by L. G. Christophorou, E. Illenberger, and W. F. Schmidt (Plenum, New York, 1994), p. 339.
[15] P. Krebs and U. Lang, J. Phys. Chem. **100**, 10482 (1996).
[16] A. N. Asaad, Th. Klahn, and P. Krebs, J. Chem. Phys. **105**, 8633 (1996).
[17] P. Krebs and St. Vautrin, J. Phys. IV (Paris), Colloq. C5, Suppl. **1**, 115 (1991).
[18] P. Mikulski, Th. Klahn, and P. Krebs, Phys. Rev. A **55**, 369 (1997).
[19] C. Desfrançois, H. Abdoul-Carime, N. Khelifa, and J. P. Schermann, J. Chim. Phys. (Paris) **92**, 409 (1995).
[20] J. A. Stockdale, F. J. Davis, R. N. Compton, and C. E. Klots, J. Chem. Phys. **60**, 4279 (1974).
[21] Landolt Börnstein, Neue Serie, Gr. 2., Vol. 19c (Springer, Berlin, Heidelberg, 1992).
[22] Th. Klahn and P. Krebs, Ber. Bunsenges. Phys. Chem. **98**, 1630 (1994).
[23] A. Ya. Polischuk, Phys. Lett. **110A**, 103 (1985).
[24] A. Ya. Polischuk, J. Phys. B **18**, 829 (1985).
[25] Th. Klahn, Doctoral thesis, University of Karlsruhe, 1995.
[26] P. Manicke, Chemiker-Zeitung, Germany **50**, 333 (1926).
[27] D. Hummel and O. Jannsen, Z. Phys. Chem. (Munich) **31**, 111 (1962).
[28] *Gmelins Handbook of Inorganic Chemistry, Carbon, Part D,* 8th ed. (Verlag Chemie, Weinheim/Bergstr., Germany, 1971), p. 199.
[29] T. Aoyama, Japan Soc. High Pressure Gas Ind. **19**, 121 (1955).
[30] A. Sporzynski and H. L. Slater, Recl. Trav. Chim. Pays-Bas. **69**, 619 (1950).
[31] Thermodynamic Research Center 1972, *Selected Values of Properties of Chemical Compounds,* Texas A&M University, Vol. I, Table 23-18-2-(1.0213)-h.
[32] Th. Klahn and P. Krebs, J. Chem. Phys. **109**, 543 (1998), following paper.
[33] For example, note some critical comments in the publication of P. W. Adams, D. A. Browne, and M. A. Paalanen, Phys. Rev. B **45**, 8837 (1992).
[34] S. Altshuler, Phys. Rev. **107**, 114 (1957).
[35] H. Sinosaki and R. Hara, Tech. Rep. Tohoku Univ. (Japan) **8**, 297 (1929).
[36] W. A. Felsing and G. W. Drake, J. Am. Chem. Soc. **58**, 1714 (1936).
[37] C. F. Curtiss and J. O. Hirschfelder, J. Chem. Phys. **10**, 491 (1942).
[38] W. F. Giauque and R. A. Ruehrwein, J. Am. Chem. Soc. **61**, 2626 (1939).
[39] G. E. Hyde and D. F. Hornig, J. Chem. Phys. **20**, 647 (1952).
[40] W. J. Jones, R. M. Seel, and N. Sheppard, Spectrochim. Acta A **25**, 385 (1969).
[41] H. D. Mettee, J. Phys. Chem. **77**, 1762 (1973).

[42] A. C. Legon, D. J. Millen, and P. J. Mjöberg, Chem. Phys. Lett. **47**, 589 (1977).
[43] R. D. Brown, P. D. Godfrey, and D. A. Winkler, J. Mol. Spectrosc. **89**, 352 (1981).
[44] E. J. Campbell and S. G. Kukolich, Chem. Phys. **76**, 225 (1983).
[45] M. Kofranek, H. Lischka, and A. Karpfen, Mol. Phys. **61**, 1519 (1987).
[46] M. Kofranek, H. Lischka, and A. Karpfen, Chem. Phys. **113**, 53 (1987).
[47] R. S. Ruoff, J. Chem. Phys. **94**, 2717 (1991).
[48] L. G. Christophorou, G. S. Hurst, and W. G. Hendrick, J. Chem. Phys. **45**, 1081 (1966).
[49] R. A. Young, Phys. Rev. A **2**, 1983 (1970).
[50] J. M. Warman, M. P. deHaas, and A. Hummel, in *Proceedings of the 5th International Conference on Conduction and Breakdown in Dielectric Liquids*, edited by J. M. Goldschwartz (Delft University Press, Delft, 1975), p 70.
[51] K. Itoh and R. Holroyd, J. Phys. Chem. **94**, 8850 (1990); **94**, 8854 (1990).
[52] K. G. Mothes, E. Schultes, and R. N. Schindler, Ber. Bunsenges. Phys. Chem. **76**, 1258 (1972).
[53] C. Desfrançois, H. Abdoul-Carime, C. Adjouri, N. Khelifa, and J. P. Schermann, Europhys. Lett. **26**, 25 (1994).
[54] K. D. Jordan and J. J. Wendoloski, Chem. Phys. **21**, 145 (1977).
[55] T. R. Dyke and J. S. Muenter, J. Chem. Phys. **60**, 2929 (1974).
[56] C. Desfrançois, B. Baillon, J. P. Schermann, S. T. Arnold, J. H. Hendricks, and K. H. Bowen, Phys. Rev. Lett. **72**, 48 (1993).
[57] Landolt Börnstein, Neue Serie, Gr. 2., Vol. 6 (Springer, Berlin, Heidelberg 1974).
[58] N. Hamilton and J. A. D. Stockdale, Aust. J. Phys. **19**, 813 (1966).
[59] A. D. Buckingham and R. E. Raab, J. Chem. Soc. **4**, 5511 (1961).